IJNRD.ORG ISSN : 2456-4184
INTERNATIONAL JOURNAL OF NOVEL RESEARCH AND DEVELOPMENT (IJNRD) | IJNRD.ORG
An International Open Access, Peer-reviewed, Refereed Journal

Fundamental Characteristics of Gold Nanoparticles and Their Role in Tumor Diagnosis and Treatment

Aman Yadav[1]*, Siddharth kowsik[1], Abhash Singh[1], Ankita Patel[2]

Department of Pharmaceutics, Shambhunath Institute Of Pharmacy, Prayagraj[1] &
Malti Memorial Trust CSM "Group of Institution" Faculty of B.Pharmacy, Prayagraj[2]

ABSTRACT

Gold nanoparticles (AuNPs) have garnered significant attention in the realm of tumor diagnosis and treatment due to their unique fundamental properties. To optimize AuNPs for these applications, it is essential to thoroughly understand their inherent characteristics and their interconnectedness.

AuNPs possess distinct physical and chemical properties that are pivotal in their utility. Physically, AuNPs exhibit localized surface plasmon resonance (LSPR), high X-ray absorption coefficient, and radioactivity, which are extensively leveraged in tumor diagnosis and therapy. Chemically, AuNPs can form stable bonds with sulfur (S) and nitrogen (N)-containing groups, facilitating versatile surface modifications with organic ligands or polymers tailored for specific functions. These modifications enhance AuNPs' biocompatibility, targeting efficiency, and drug delivery capabilities.

This review systematically summarizes the physicochemical properties of AuNPs and elucidates their intrinsic relationships. It also discusses recent advancements in research and clinical trials utilizing these properties. Furthermore, the review identifies challenges in translating laboratory findings to clinical applications and proposes potential solutions. Finally, it assesses the feasibility of integrating these findings into clinical trials, aiming to guide researchers in effectively harnessing the remarkable physicochemical properties of gold nanoparticles for oncological therapies.

1. Introduction

The historical use of gold nanoparticles (AuNPs) in biomedicine dates back to the Middle Ages, where "potable gold," known in old Latin texts as "aurum potabile," was believed to possess remarkable therapeutic properties against ailments such as heart and venereal diseases, arthritis, epilepsy, and tumors, and even for diagnosing syphilis [1]. However, due to limited understanding at the time, the colloidal gold used was often in an oxidized state, leading to significant side effects during its application.

Modern nanotechnology has revolutionized the biomedical applications of AuNPs, leading to substantial progress and continued research interest in their potential. Several reviews have highlighted the superior properties of AuNPs and their diverse biomedical applications. For instance, Ghosh and Pal discussed the interparticle coupling effect on the surface plasmon resonance (SPR) of AuNPs, focusing on assembling strategies, optical properties, and applications [2]. In contrast, Dreaden et al. emphasized the synthesis, functionalization, and in vivo metabolic dynamics of AuNPs across diagnostics, imaging, and medicine [3]. Dykman and Khlebtsov explored the immunological properties of AuNPs, while Yang et al. covered their chemical synthesis, optical properties, biomedical applications, and pharmacokinetics, with a particular focus on tunable optical properties [4, 5].

The physical and chemical properties of AuNPs, influenced significantly by their nanostructure (shape and crystal texture), play a crucial role in their biomedical applications. For instance, gold nanorods or nanostars are preferred for photothermal therapy (PTT) or photodynamic therapy (PDT) due to their efficient absorption of near-infrared light (NIR) compared to spherical AuNPs [6]. Additionally, Au clusters have unique capabilities, such as producing propylene oxide (PO) from O2 and water, which AuNPs cannot achieve [7].

In the context of tumor diagnosis and treatment, understanding the natural properties of AuNPs is essential for optimizing their application. This review focuses on elucidating these fundamental properties—both physical and chemical—and their interrelationships. These properties include their roles as imaging agents, in phototherapy, radiotherapy, targeting, nano-enzyme applications, and drug delivery (Figure 1). Clinical trials showcasing AuNPs with various physical and chemical properties are highlighted to provide insights into their potential for clinical translation.

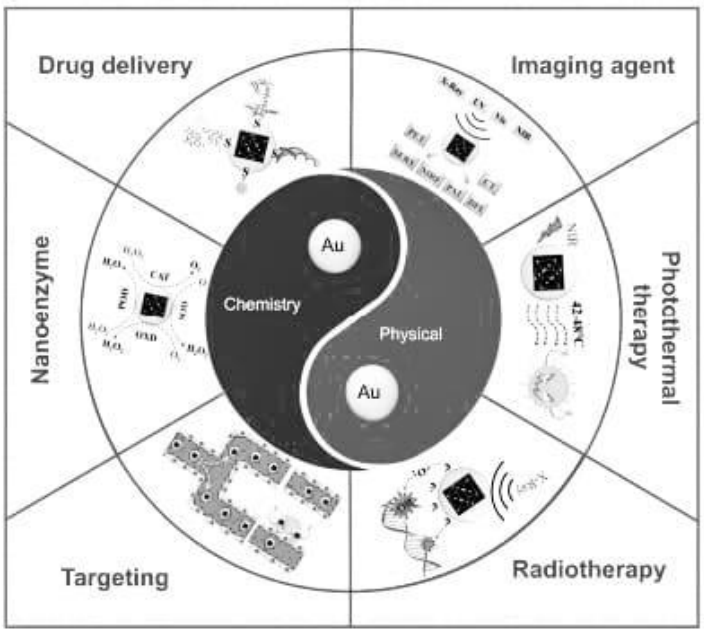

Figure 01 Applications for tumor diagnosis and treatment based on the basic physical and chemical properties of gold nanoparticles

2. Characteristics of AuNPs

The physical properties of gold nanoparticles (AuNPs)—localized surface plasmon resonance (LSPR), radioactivity, and high X-ray absorption coefficient—are pivotal in both diagnosing and treating tumors. LSPR in AuNPs enables various applications such as surface-enhanced Raman spectroscopy (SERS), surface-enhanced fluorescence (SEF), photothermal and photochemical conversions, and colorimetric responses. These capabilities

are extensively utilized for non-invasive detection in vivo and in situ, as well as for imaging, photothermal therapy (PTT), photodynamic therapy (PDT), and in vitro diagnostics (IVD).

The radioactivity of AuNPs is harnessed for radiotherapy and radionuclide imaging (RNI), further enhancing their role in cancer treatment. Additionally, the high atomic number of AuNPs enhances their effectiveness in radiotherapy by sensitizing tumor cells.

These unique physical properties highlight the versatility of AuNPs in oncology applications, significantly advancing diagnostic accuracy and therapeutic efficacy in the field.

2.1. Localized Surface Plasmon Resonance (LSPR)

Under light stimulation, electrons on a noble metal collectively oscillate, a phenomenon known as "plasmon" [8]. Plasmon resonance (PR) occurs when incident photons resonate with these oscillations of conduction electrons [6]. Due to rapid attenuation of the incident electromagnetic wave within the metal, resonance predominantly occurs at the metal surface, termed surface plasmon resonance (SPR) [9]. When SPR occurs in nanoparticles (NPs), which are similar in size to the incident light wavelength, it is termed localized surface plasmon resonance (LSPR). LSPR in gold nanoparticles (AuNPs) induces two significant effects: enhancement of the local electromagnetic field and increased extinction coefficient (Figure 2).

During LSPR, electromagnetic fields near the surface of AuNPs can undergo significant enhancement, particularly in regions of high local curvature known as "hot spots" [10]. These hot spots amplify the spectral signals of nearby substances, a phenomenon referred to as surface enhancement spectroscopy (SES), crucial in oncotherapy applications such as surface-enhanced Raman spectroscopy (SERS) and surface-enhanced fluorescence (SEF) [11].

Moreover, LSPR maximizes the optical extinction of AuNPs (e.g., 2.7 × 10^8 M^–1 cm^–1 for 13 nm AuNPs), over 1000 times stronger than typical organic molecules [12]. This enhancement significantly boosts the efficiency of photothermal and photochemical conversions, as well as light energy absorption by AuNPs. These properties are exploited in photothermal therapy (PTT), photodynamic therapy (PDT), and colorimetric assays for tumor diagnosis and treatment.

This section emphasizes the physical properties of AuNPs influenced by LSPR and their intricate relationship. Factors such as nanoparticle size, shape, composition, and microenvironment profoundly impact LSPR characteristics. For further exploration, interested readers are encouraged to refer to comprehensive reviews cited in Reference [13]

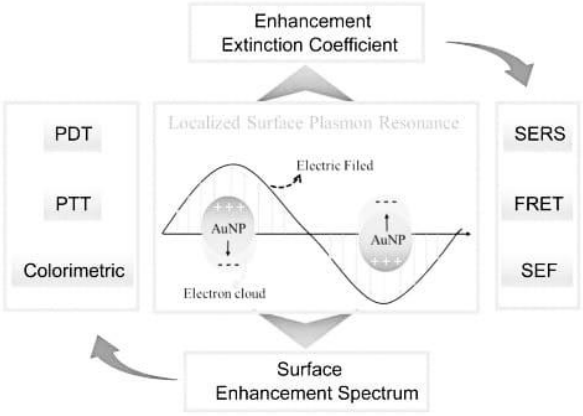

Figure 02 Localized surface Plasmon resonance of AuNPs and associated properties.

2.1.1. Surface-Enhanced Raman Spectroscopy

When monochromatic light interacts with a particle, Rayleigh scattering occurs if the particle is significantly smaller than the wavelength of the light. According to theory, the scattered light retains the same frequency and direction as the incident light. However, molecules adsorbed on the particle's surface also vibrate upon absorbing light, causing some of the scattered light to deviate in frequency from the original incident light. This phenomenon results in both Stokes scattering (lower energy) and anti-Stokes scattering (higher energy). The difference in energy between the scattered photon and the incident photon is known as Raman scattering (RS) [14]. RS corresponds to the vibrational mode energy of the adsorbed molecule, making Raman imaging capable of providing finely detailed vibrational information (approximately 0.1 nm resolution), often referred to as a "chemical fingerprint," crucial for precise single molecule detection [15].

However, the cross-sections of RS are typically small, ranging from 10 to 30 cm^2/molecule, which limits its sensitivity and detectability [16]. This limitation is overcome by surface-enhanced Raman spectroscopy (SERS), which can enhance Raman signals from 10^6 to 10^{15}, significantly boosting signal sensitivity. SERS finds extensive use in sensing, detection, and imaging applications, particularly in cancer diagnosis [17]. Gold nanoparticles (AuNPs) serve as effective contrast agents in SERS, facilitating imaging of small tumors, differentiation of tumor cells, monitoring of tumor metabolism, and detection of tumor markers.

For instance, Qian et al. employed AuNPs conjugated with single-chain variable fragment (ScFv) antibodies targeting epidermal growth factor receptors (EGFR) on human cancer cells and xenograft tumor models, successfully enhancing and detecting RS signals [18]. Hossain et al. utilized an AuNP-deposited ITO substrate to enhance Raman signals, effectively characterizing and distinguishing sub-types of breast cancer cells originating from various organs [19]. Shiota et al. utilized AuNPs with horse-bean shapes to generate multiple SERS excitation sources, visualizing hypotaurine consumption, a critical mechanism in cancer survival [20]. Lin et al. demonstrated the diagnostic utility of AuNP-based SERS in detecting colorectal tumor markers with high sensitivity and specificity in patient serum samples [21].

For further insights into the application of AuNPs as SERS imaging agents, interested readers are encouraged to explore additional literature reviews (e.g., [22]).

2.1.2. Surface Enhanced Fluorescence

Localized Surface Plasmon Resonance (LSPR) in AuNPs can induce either fluorescence quenching or enhancement in fluorescent molecules, depending on their proximity to the nanoparticles. When free fluorescent molecules absorb photons, they transition from the ground state to an excited state. Subsequently, they undergo vibrational relaxation and internal conversion (k_int), followed by returning to the ground state through energy decay, which includes radiative decay (γ) and nonradiative decay (k_nr) rates, where radiative decay manifests as fluorescence emission [23].

Nonradiative decay processes include intersystem transitions and energy transfer mechanisms like fluorescence resonance energy transfer (FRET), which predominantly causes fluorescence quenching in the presence of AuNPs. FRET efficiency decreases sharply with distance, and when the distance is less than 5 nm, the excited state energy of fluorescent molecules transfers completely to AuNPs, resulting in quenching [24]. This interaction between AuNPs and fluorescent molecules is pivotal for diagnostic applications, often achieved by linking them with specific linkers that modulate their spatial relationship. For instance, recognition sequences in linkers are employed to target cancer cells in lung tumors, acute lymphocytic leukemia, human Burkitt's lymphoma, and for detecting intracellular mRNA in cancer cells [25-29].

Conversely, LSPR can enhance fluorescence via two mechanisms: improving the excitation efficiency and increasing the radiative decay rate of fluorescence. Enhanced electromagnetic fields at "hot spots" on AuNPs intensify molecule excitation, while AuNPs act as resonant cavities that elevate the radiative rate of quantum

emitters by enhancing the local density of states [30]. This property makes AuNPs valuable in applications such as two-photon luminescence (TPL) imaging for tumor cell visualization and three-dimensional in vivo imaging [31, 32]. AuNPs also facilitate connections with quantum dots, fluorescent molecules, or cellular autofluorescence emission, thereby enhancing tumor cell detectability and guiding targeted tumor therapy [33].

2.1.3. Photothermal Conversion

After absorbing photons, AuNPs convert the energy of light into kinetic energy of electrons. These energetic electrons interact with the lattice/phonons of the material, causing them to scatter and transfer some of their kinetic energy into lattice vibrations. Ultimately, this vibrational energy dissipates as heat, which is known as the "photothermal effect."

In cancer therapy, this effect is particularly advantageous due to the unique characteristics of tumor vasculature, which often lacks efficient blood vessel structure, leading to poor heat dissipation. Consequently, heat generated by photothermal conversion tends to accumulate within tumors, raising their temperature significantly (up to 46°C), while surrounding normal tissues typically reach temperatures around 41°C. Tumor cells are also more susceptible to heat compared to normal cells, with lethal temperatures for tumors generally being between 42.5°C to 43°C, whereas normal cells can tolerate temperatures as high as 47°C. This differential thermal sensitivity makes photothermal conversion a promising approach for cancer cell imaging and photothermal therapy (PTT) [34].

Biological tissues exhibit low absorption and negligible spontaneous fluorescence in the near-infrared (NIR) spectrum [35], making it an ideal range for PTT applications. By adjusting the surface plasmon resonance of AuNPs to the NIR region, efficient photothermal conversion can be achieved, termed as plasmonic photothermal therapy (PPTT) [36]. Initially demonstrated in vitro using visible light in 2003, AuNPs have since been successfully applied in vivo for PTT via interstitial and intravenous injections [37-39]. Numerous strategies have been developed to enhance the efficiency of photothermal conversion and optimize AuNP performance for in vivo applications, including aggregation of small AuNPs (<10 nm) and nanostructure modifications [40].

Monitoring the photothermal conversion of AuNPs can be achieved through techniques such as photothermal imaging (PTI) [34] and photoacoustic imaging (PAI). These methods are instrumental in clinical tumor diagnosis, aiding in hyperthermia procedures and integrating visual therapy with diagnostic capabilities [42]. For further details on the applications and principles of AuNPs in PTT and PAI, additional references are available [43].

2.1.4. Photosensitization

In response to photoexcitation, gold nanoparticles (AuNPs) can transfer their excited state photon energy to nearby molecules, such as organic photosensitizers or molecular oxygen (O2). This process leads to the generation of cytotoxic oxygen-based species like singlet oxygen (1O2), $O2^-$, and OH^-, which are crucial in photodynamic therapy (PDT) for cancer treatment [44]. AuNP-based PDT involves two main approaches: (1) using AuNPs to enhance the photosensitization of existing photosensitizers to produce 1O2, and (2) AuNPs acting as photosensitizers themselves to directly generate 1O2.

Due to their localized surface plasmon resonance (LSPR), AuNPs efficiently absorb near-infrared (NIR) light energy and transfer it to photosensitizers or molecular oxygen. This capability addresses limitations of conventional organic photosensitizers, such as poor stability and low light energy conversion efficiency [45]. As a photosensitizer enhancer, AuNPs can enhance the sensitization of organic photosensitizers to produce 1O2 [46]. Alternatively, AuNPs can directly sensitize molecular oxygen to generate 1O2, effectively killing tumor cells [47].

In pioneering work, Vankayala and colleagues demonstrated that AuNPs can sensitize 1O2 formation under visible and NIR light excitation, showing significant PDT efficacy in treating solid tumors in animal models [48]. The yield of 1O2 formation has been linked to the shape of AuNPs [49]. Ongoing research focuses on enhancing AuNP roles in PDT. For instance, Chen et al. developed an AuNP-based photosensitizer capable of fluorescence imaging, alleviating tumor hypoxia, and inducing PDT under NIR-II (1064 nm) light in vivo [50].

PTT and PDT are frequently combined in studies, leveraging their complementary strengths in cancer therapy. The applications of these combined therapies are summarized in Table 1.

Table 01 AuNPs are used for photodynamic therapy (PDT) and photothermal therapy (PTT) combination

Gold Nanostructure	Laser (nm)	Coating	Application	Reference
Nanocages	940	Lipid	Hela; PTT/PDT	[51]
Nanocages	980	Lipid	B16F0 melanoma tumors	[51]
Nanocages	790	Hypocrellin and Lipid	Hela; PTT/PDT	[52]
Nanostar	671	Chlorin e6	breast cancer and lung cancer; PTT/PDT	[53]
Nanorods	808	Styrene-alt-maleic acid Indocyanine green	anti-EGFR antibody; PTT/PDT	[54]
Nanorods	810	Rose bengal	Hamster cheek pouches; PTT/PDT	[55]
Nanorods	770	Ce6–pHLIPss Thiol-terminated monomethoxyl	95-C cells; PTT/PDT	[56]
Nanorod	633 and 808	Mesoporous silica Hematoporphyrin	large solid tumors; PTT/PDT	[57]
Nanorods	808+633	Neutrally charged polymers	white outbred male rats with implanted cholangiocarcinoma PC-1; PTT/PDT	[58]
Nanorods	670–710	Sulfonated aluminum Phthalocyanines	human nasopharyngeal carcinoma cells; PTT/PDT	[59]
Nanorod	810 and 670 subsequently	AlPcS4	xenografted mouse tumor; PTT/PDT	[60]
Hollow gold nanospheres	670	pHLIP and Ce6	Hela; PTT/PDT	[61]

2.1.5. Colorimetric Responses

Due to their high molar absorption coefficient, gold nanoparticles (AuNPs) enable highly sensitive detection through colorimetric analysis at nanomole levels, significantly surpassing traditional methods. AuNP-based assays exploit the plasmon-induced color change from red to blue, purple, or gray upon analyte-induced aggregation of AuNPs. These analytes encompass tumor-related proteins, nucleic acids, and cytokines [62]. Kang et al. pioneered the application of AuNP-based colorimetric assays for cancer diagnosis in 2010, focusing on charge-induced AuNP aggregation using activated protein kinase Cα (PKCα) as a cancer marker [63]. They employed a cationic PKCα-specific peptide substrate and AuNPs with anionic surface charges as the chromogenic agent. Phosphorylation of the cationic peptide substrate in cancer cells or tissue lysates increased anionic charges at the phosphorylation site, inhibiting AuNP aggregation and maintaining a red color. Conversely, normal cells or tissue lysates resulted in a blue color.

Furthermore, Lu et al. demonstrated the selective detection of breast cancer with high HER2 expression using antibody-induced AuNP aggregation [65]. Lee et al. utilized AuNP-based assays for ultra-selective detection of

cancer mutations (e.g., BRCA1, EGFR, KRAS, p53) through base pairing-induced AuNP aggregation [66]. This platform supports signal amplification via isothermal amplification or polymerase chain reaction, achieving visualization of cancer-related molecules with picomolar sensitivity suitable for point-of-care applications [68, 70]

2.2. Radioactivity

Gold (Au) is a metal with radionuclide properties that make it valuable in biomedicine. Isotopes like 198Au (half-life of 2.7 days) and 199Au (half-life of 3.2 days) are used because they can be excreted intact in urine [71] or accumulate in the liver [72]. These isotopes emit β-particles with energies of 0.96 MeV (198Au) and 0.45 MeV (199Au), along with γ-rays (412 keV for 198Au and 208 keV for 199Au), which are useful for imaging [73].

198AuNPs, enriched with these radioactive isotopes, require smaller quantities to achieve therapeutic levels of radioactivity [74]. The high-energy β-emission of 198AuNPs is effective for tumor cell destruction [75], as demonstrated in studies where intravenous injection of 198AuNPs inhibited tumor growth significantly in mouse models of prostate cancer [76]. Target-specific 198AuNPs have been developed to enhance tumor accumulation, using tumor-specific antibodies or nanocomposite devices [76].

The γ-rays emitted by AuNPs can penetrate soft tissues effectively, making them suitable for imaging using single-photon emission computed tomography (SPECT) scanners [77]. For instance, PEGylated 198AuNPs have been used to image AuNPs in living animals and dissected tissues [79], and they have also been employed in Cerenkov luminescence imaging [80].

199Au, emitting β-particles with a maximum energy of 0.45 MeV and γ-rays of 208 keV, is particularly suitable for SPECT imaging [81]. This isotope has been incorporated into AuNPs for imaging in clinical studies, such as in mouse models of triple-negative breast cancer [82]. Researchers have also explored using 198,199Au-labeled amino-functionalized graphene oxide sheets for SPECT imaging in rat models of fibrosarcoma tumors [83].

The use of 199AuNPs is advantageous due to their ability to selectively bind to monoclonal antibodies, enhancing tumor targeting and potentially increasing therapeutic efficacy [84]. For further insights into the role of AuNPs in tumor imaging and treatment, relevant reviews can be consulted [85].

2.3. High Atomic Number

When the atomic number exceeds 53, the absorption of X-rays increases [86]. Gold (Au), with an atomic number of 79, exhibits a significantly enhanced X-ray absorption coefficient [87]. This property makes Au promising as a sensitizer in radiotherapy for oncological treatments [88]. AuNPs enhance the cross-section of cancer cells or tissues to X-rays and emit secondary electrons such as photoelectrons [89], Auger electrons [90], Compton electrons [91], and other forms, which can directly ionize DNA molecules. This ionization leads to breaks in DNA strands, cross-linking of bases and sugars [93], and the generation of free radicals through interaction with tissue water [94]. These radicals bind to DNA, initiating electron transfers that further oxidize target DNA molecules.

The mechanism behind AuNP-mediated radiotherapy sensitization is often quantified using a dose enhancement factor (DEF) [95]. The DEF of AuNPs depends on various factors including nanoparticle diameter, concentration, X-ray energy, intracellular localization, and the three-dimensional distribution of radiation doses [96-99]. Initial experiments by Hainfeld et al. underscored the radiosensitization effect of AuNPs, demonstrating prolonged survival in tumor-bearing mice treated with radiotherapy and AuNPs [100].

In addition to sensitizing radiotherapy, AuNPs' high X-ray absorption rate makes them effective contrast agents for X-ray (CT) imaging in cancer diagnosis, treatment guidance, and therapeutic evaluation. Popovtzer et al.

pioneered molecular CT imaging of cancer using targeted AuNPs, showing clear visualization of small tumor tissues in vivo [101, 102]. By modifying AuNPs with antibodies such as anti-EGFR, they achieved targeted imaging in models of head and neck cancer.

For a comprehensive understanding of the theory and applications of gold nanoparticles in tumor radiotherapy, refer to detailed reviews [95], which discuss the physics, chemistry, and biological mechanisms of AuNP radiosensitization

3. Chemical Properties

3.1. Easy to Couple

Gold nanoparticles (AuNPs) possess a distinct advantage over numerous other nanoparticles due to their ability to establish stable chemical bonds with groups containing sulfur (S) and nitrogen (N). This unique characteristic enables AuNPs to conjugate effectively with a diverse range of organic ligands or polymers tailored for specific functionalities. These surface modifications significantly enhance the biocompatibility of AuNPs and equip them with exceptional capabilities for targeting specific sites and delivering drugs [103].

3.1.1. Biocompatibility

The biocompatibility of gold nanoparticles (AuNPs) in vivo is evaluated through their pharmacokinetics, tissue distribution, toxicity, and clearance mechanisms. Achieving biocompatibility is crucial for all applications of AuNPs in vivo, which can be enhanced by surface modifications, primarily through the formation of stable Au–S bonds.

Strategies to optimize the pharmacokinetics of AuNPs include prolonging their circulation half-life by reducing clearance by the mononuclear phagocyte system (MPS) or optimizing their physical size. Polyethylene glycol (PEG) is widely used to decrease AuNP uptake by the MPS, with longer PEG chains increasing circulation half-life [104]. Compared to larger AuNPs (e.g., 100 nm), smaller ones (e.g., 15 nm) exhibit prolonged in vivo circulation times [105]. However, AuNPs smaller than 6 nm are rapidly filtered and cleared by the kidneys [106].

For applications in tumor diagnosis and treatment, AuNPs must enhance retention in tumor tissues while minimizing accumulation in other organs. Upon entering circulation, AuNPs quickly undergo opsonization, leading to the formation of a protein corona that facilitates recognition by phagocytic cells in the MPS, predominantly located in the liver, spleen, and bone marrow [107]. Charged surfaces of AuNPs are more prone to forming protein coronas compared to neutral surfaces [40]. Accumulation of AuNPs in non-target organs can lead to toxicity, characterized by acute inflammatory responses and cell apoptosis. For instance, specific sizes of AuNPs have been shown to disrupt cellular metabolism and induce adverse effects in animal models [108, 109]. Fortunately, these toxic effects can be mitigated through surface modifications and optimization of physicochemical parameters.

To minimize toxicity and enhance clearance from healthy organs, AuNPs are primarily cleared from the body via renal and biliary pathways, as they are not metabolized enzymatically within the body. Small AuNPs (less than 10 nm) are efficiently cleared via renal pathways, with up to 70% eliminated within 72 hours, while larger ones are cleared via bile [110, 111]. Although the exact mechanisms remain under investigation, studies have consistently demonstrated the clearance mechanisms of AuNPs from the body.

For further detailed information on AuNP biocompatibility and clearance mechanisms, interested readers are encouraged to consult relevant reviews [5, 6, 112].

3.1.2. Targeting

Targeting strategies for gold nanoparticles (AuNPs) can be categorized into passive targeting, involving the enhanced permeability and retention (EPR) effect and mononuclear phagocyte system (MPS) escape, and active targeting, which includes tumor cell-specific targeting and stimuli-responsive targeting. The EPR effect takes advantage of the abnormal vasculature and limited lymphatic drainage in tumors due to their rapid growth, allowing certain-sized AuNPs to efficiently penetrate and accumulate within tumor tissues. This property has been exploited for both imaging and therapeutic applications in cancer [113, 114].

MPS escape strategies for AuNPs often involve surface coatings with hydrophilic polymers [115], branched architectures [116], or particles with both hydrophilic and hydrophobic domains [117]. These modifications help evade immune system recognition and clearance, thereby enhancing AuNP accumulation at tumor sites.

Active targeting of AuNPs relies on specific ligands that can recognize and bind to receptors overexpressed on cancer cells. Examples include Lam 67R and GRP for human prostate tumors [85, 118], and CCR5 and HER2 for breast tumors [65]. These ligand-functionalized AuNPs improve specificity and efficacy in targeting cancer cells while minimizing off-target effects.

Stimuli-responsive targeting involves both exogenous stimuli such as near-infrared (NIR) light [119], magnetic fields [120], and ultrasound [121], as well as endogenous stimuli such as pH changes [56] and redox conditions [122]. These stimuli trigger controlled release of therapeutic payloads from AuNPs within the tumor microenvironment, enhancing treatment efficacy while reducing systemic side effects.

3.1.3. Delivery

Gold nanoparticles (AuNPs) exhibit a capability to combine with chemotherapy drugs, proteins, or nucleic acids through electrostatic adsorption or covalent bonds. This property, coupled with their excellent biocompatibility and targeting abilities, positions them as highly promising vehicles for tumor-targeted delivery. In chemotherapy, AuNPs can effectively carry drugs such as mitoxantrone (MTX) [123], phthalocyanine4 (Pc4) [124], doxorubicin (Dox) [125], and photosensitizers [46], thereby enhancing their accumulation at tumor sites and improving therapeutic outcomes.

In immunotherapy, AuNPs can be loaded with immune-targeting antibodies to stimulate immune cell activation. Examples of these antibodies include polyclonal anti-carcino-embryonic antigen (CEA) [126], monoclonal anti-HER2 [121], among others. Dumani et al. developed AuNPs coated with glycol-chitosan that facilitate uptake by immune cells and subsequent transport to sentinel lymph nodes for metastasis detection [121].

3.2. Catalytic Activity and Applications

In 1987, Haruta et al. published pioneering research demonstrating that gold nanoparticles (AuNPs) exhibit exceptional efficiency in catalyzing the oxidation of carbon monoxide (CO) at or below room temperature [128]. This discovery sparked rapid development in the field of AuNP-based biomimetic catalysts [129]. Since then, AuNPs have been shown to mimic the activities of various enzymes including nucleases, esterases, silicatein, glucose oxidase (GO), peroxidase (POD), catalase, superoxide dismutase, and oxidase.

Among these mimic enzyme activities, the peroxidase-like activity of AuNPs was initially observed by catalyzing the oxidation of the peroxidase substrate 3,3,5,5-tetramethylbenzidine (TMB) using hydrogen peroxide (H_2O_2), resulting in a blue color formation in aqueous solutions [130]. This capability has been utilized to catalyze H_2O_2 within tumor cells under acidic conditions to generate hydroxyl radicals (·OH), inducing

intracellular oxidative damage in gastric tumors [131], and to detect glutathione (GSH) concentrations for cancer diagnostics [132].

The glucose oxidase-like activity of AuNPs involves the aerobic oxidation of glucose to gluconate and H2O2, which serves as a model reaction [133]. The localized production of H2O2 can trigger the growth of AuNPs, enabling sensitive detection of cancer biomarkers at picomolar levels [134]. Moreover, H2O2 produced can also act as a substrate for POD-like catalysis, leading to the generation of highly toxic hydroxyl radicals that induce apoptosis in tumor cells [135].

3.3. Biological Activity

Gold nanoparticles (AuNPs) possess intrinsic antineoplastic biological activity in addition to their role in tumor therapy through external functionalization or activation. This biological activity is often size-dependent, with smaller AuNPs (less than 2 nm) capable of inducing cellular oxidative stress, mitochondrial damage, and interactions with DNA, thereby causing cancer cell death. Larger AuNPs do not exhibit the same cytotoxic effects at equivalent concentrations [136].

AuNPs with a particle size around 5 nm selectively interact with heparin-binding glycoproteins on endothelial cell surfaces, altering their molecular conformation and inhibiting tumor activity [137]. Furthermore, AuNPs have been reported to enhance apoptosis and suppress the proliferation of cancer cells [138]. They also selectively accumulate in the mitochondria of tumor cells, where they reduce mitochondrial membrane potential, increase reactive oxygen species production, and ultimately induce apoptosis in tumor cells. Importantly, normal cells and stem cells do not demonstrate the same susceptibility to these effects [139].

4. Application of AuNPs in Clinical Trial

In practical applications, particularly in clinical trials, a comprehensive utilization of the physical and chemical properties of gold nanoparticles (AuNPs) is crucial to achieve effective oncotherapy. The current clinical trial applications of AuNPs are summarized in Table 2.

Table 02 AuNPs are used for clinical trials in tumor therapy and diagnosis

Name	Composition	Physical& Chemical Property	Application	Phases	Ref.
CYT-6091 (Aurimune)	AuNsphere rhTNF tPEG	Delivery	Melanoma Sarcoma	PhaseIcomplete	[140]
Aurolase® therapy	AuNshell Silica PEG	EPR effect Photothermal conversion	Head and Neck Cancer, Lung Tumors, Prostate Cancer	Not Applicable	[141]
PEGylated gold nanoparticles	AuNRod PEG	Photothermal conversion	Deep-tissue Malignancies	Human pilot studies	[142]
NU-0129	Spherical Nucleic Acid Ausphere	Delivery	Glioblastoma Gliosarcoma	Early Phase I	[143]

5. Areas for Improvement and Future Directions

Despite the abundant promising data from laboratory studies, there is a notable scarcity of gold nanoparticle (AuNP)-based tumor therapy strategies currently undergoing or entering clinical trials. This gap is primarily

attributed to several challenges encountered during the transition from laboratory research to clinical application. These challenges include overcoming the clearance mechanisms of the mononuclear phagocytic system (MPS) and renal excretion to effectively target tumor tissues, navigating through various physiological barriers to exert therapeutic effects, and understanding the metabolic fate of nanoparticles post-treatment.

A promising approach to address these challenges involves optimizing the utilization of AuNPs' physical and chemical properties. For instance, Liu and colleagues devised a multifunctional poly(amino acid)–gold–magnetic complex characterized by its large particle diameter (~170 nm), enabling evasion of renal clearance. The complex utilizes the enhanced permeability and retention (EPR) effect to penetrate vascular barriers, facilitating efficient CT imaging due to its high X-ray absorption coefficient. Moreover, its guanidine group enhances uptake efficiency by coupling with arginine on AuNPs, while its high photothermal conversion capability allows for effective photothermal therapy (PTT). Crucially, the complex biodegrades into smaller particles (~3 nm), enabling renal clearance post-therapy.

By leveraging these exceptional properties of AuNPs through innovative designs, it is anticipated that more AuNP-based tumor therapy strategies will advance into clinical trials and ultimately receive approval for treating cancer patients.

REFERENCES

1. Higby, G.J. Gold in medicine: A review of its use in the West before 1900. Gold Bull. 1982, 15, 130–140.
2. Ghosh, S.K.; Pal, T. Interparticle Coupling Effect on the Surface Plasmon Resonance of Gold Nanoparticles: From Theory to Applications. Chem. Rev. 2007, 107, 4797–4862.
3. Dreaden, E.C.; Alkilany, A.; Huang, X.; Murphy, C.; El-Sayed, M.A. The golden age: Gold nanoparticles for biomedicine. Chem. Soc. Rev. 2011, 41, 2740–2779.
4. Dykman, L.; Khlebtsov, N.G. Gold nanoparticles in biomedical applications: Recent advances and perspectives. Chem. Soc. Rev. 2012, 41, 2256–2282.
5. Yang, X.; Yang, M.; Pang, B.; Vara, M.; Xia, Y. Gold Nanomaterials at Work in Biomedicine. Chem. Rev. 2015, 115, 10410–10488. [CrossRef]
6. Jauffred, L.; Samadi, A.; Klingberg, H.; Bendix, P.M.; Oddershede, L.B. Plasmonic Heating of Nanostructures. Chem. Rev. 2019, 119, 8087–8130. [CrossRef]
7. Ishida, T.; Murayama, T.; Taketoshi, A.; Haruta, M. Importance of Size and Contact Structure of Gold Nanoparticles for the Genesis of Unique Catalytic Processes. Chem. Rev. 2019, 120, 464–525. [CrossRef]
8. Maier, S.A.; Atwater, H.A. Plasmonics: Localization and guiding of electromagnetic energy in metal/dielectric structures. J. Appl. Phys. 2005, 98, 011101. [CrossRef]
9. Schuller, J.A.; Barnard, E.S.; Cai, W.; Jun, Y.C.; White, J.S.; Brongersma, M.L. Plasmonics for extreme light concentration and manipulation. Nat. Mater. 2010, 9, 193–204. [CrossRef]
10. Moskovits, M. Surface-enhanced spectroscopy. Rev. Mod. Phys. 1985, 57, 783–826. [CrossRef]
11. Gersten, J.I. Photophysics and photochemistry near surfaces and small particles. Surf. Sci. 1985, 158, 165–189. [CrossRef]
12. De Puig, H.; Tam, J.O.; Yen, C.-W.; Gehrke, L.; Hamad-Schifferli, K. Extinction Coefficient of Gold Nanostars. J. Phys. Chem. C 2015, 119, 17408–17415. [CrossRef]
13. Shunping, Z.; Hongxing, X. Optimizing substrate-mediated plasmon coupling toward high-performance plasmonic nanowire waveguides. Acs Nano 2012, 6, 8128–8135.
14. Shuker, R.; Gammon, R.W. Raman-Scattering Selection-Rule Breaking and the Density of States in Amorphous Materials. Phys. Rev. Lett. 1970, 25, 222–225. [CrossRef]
15. Zumbusch, A.; Holtom, G.R.; Xie, X.S. Three-Dimensional Vibrational Imaging by Coherent Anti-Stokes Raman Scattering. Phys. Rev. Lett. 1999, 82, 4142–4145. [CrossRef]
16. Nie, S. Probing Single Molecules and Single Nanoparticles by Surface-Enhanced Raman Scattering. Science 1997, 275, 1102–1106. [CrossRef]
17. Lee, M.; Lee, S.; Lee, J.-H.; Lim, H.-W.; Seong, G.H.; Lee, E.K.; Chang, S.-I.; Oh, C.H.; Choo, J. Highly reproducible immunoassay of cancer markers on a gold-patterned microarray chip using surface-enhanced Raman scattering imaging. Biosens. Bioelectron. 2011, 26, 2135–2141. [CrossRef]
18. Qian, X.; Nie, S.; Champion, P.M.; Ziegler, L.D. Surface-Enhanced Raman Nanoparticles for in-vivo Tumor Targeting and Spectroscopic Detection. AIP Conf. Proc. 2010, 1267, 81.

19. Hossain, K.; Cho, H.-Y.; Choi, J.-W. Gold Nanosphere-Deposited Substrate for Distinguishing of Breast Cancer Subtypes Using Surface-Enhanced Raman Spectroscopy. J. Nanosci. Nanotechnol. 2016, 16, 6299–6303. [CrossRef]
20. Shiota, M.; Naya, M.; Yamamoto, T.; Hishiki, T.; Tani, T.; Takahashi, H.; Kubo, A.; Koike, D.; Itoh, M.; Ohmura, M.; et al. Gold-nanofève surface-enhanced Raman spectroscopy visualizes hypotaurine as a robust anti-oxidant consumed in cancer survival. Nat. Commun. 2018, 9, 1561. [CrossRef]
21. Lin, D.; Feng, S.; Pan, J.; Chen, Y.; Lin, J.; Chen, G.; Xie, S.; Zeng, H.; Chen, R. Colorectal cancer detection by gold nanoparticle based surface-enhanced Raman spectroscopy of blood serum and statistical analysis. Opt. Express 2011, 19, 13565–13577. [CrossRef]
22. Lane, L.A.; Qian, X.; Nie, S. SERS Nanoparticles in Medicine: From Label-Free Detection to Spectroscopic Tagging. Chem. Rev. 2015, 115, 10489–10529. [CrossRef]
23. Kühn, S.; Håkanson, U.; Rogobete, L.; Sandoghdar, V. Enhancement of single-molecule fluorescence using a gold nanoparticle as an optical nanoantenna. Phys. Rev. Lett. 2006, 97, 017402. [CrossRef]
24. Yun, C.S.; Javier, A.; Jennings, T.; Fisher, M.; Hira, S.; Peterson, S.; Hopkins, B.; Reich, N.O.; Strouse, G.F. Nanometal Surface Energy Transfer in Optical Rulers, Breaking the FRET Barrier. J. Am. Chem. Soc. 2005, 127, 3115–3119. [CrossRef]
25. Shi, H.; Ye, X.; He, X.; Wang, K.; Cui, W.; He, D.; Li, D.; Jia, X. Au@Ag/Au nanoparticles assembled with activatable aptamer probes as smart “nano-doctors” for image-guided cancer thermotherapy. Nanoscale 2014, 6, 8754. [CrossRef]
26. Wang, J.; Zhu, G.; You, M.; Song, E.; Shukoor, M.I.; Zhang, K.; Altman, M.B.; Chen, Y.; Zhu, Z.; Huang, C.Z.; et al. Assembly of aptamer switch probes and photosensitizer on gold nanorods for targeted photothermal and photodynamic cancer therapy. ACS Nano 2012, 6, 5070–5077. [CrossRef]
27. Han, D.; Zhu, G.; Wu, C.; Zhu, Z.; Chen, T.; Zhang, X.; Tan, W. Engineering a Cell-Surface Aptamer Circuit for Targeted and Amplified Photodynamic Cancer Therapy. ACS Nano 2013, 7, 2312–2319. [CrossRef]
28. Seferos, D.S.; Giljohann, D.A.; Hill, H.D.; Prigodich, A.E.; Mirkin, C.A. Nano-Flares: Probes for Transfection and mRNA Detection in Living Cells. J. Am. Chem. Soc. 2007, 129, 15477–15479. [CrossRef]
29. Li, N.; Chang, C.; Pan, W.; Tang, B. Inside Back Cover: A Multicolor Nanoprobe for Detection and Imaging of Tumor-Related mRNAs in Living Cells (Angew. Chem. Int. Ed. 30/2012). Angew. Chem. Int. Ed. 2012, 51, 7601. [CrossRef]
30. Fu, Y.; Zhang, J.; Lakowicz, J.R. Plasmon-Enhanced Fluorescence from Single Fluorophores End-Linked to Gold Nanorods. J. Am. Chem. Soc. 2010, 132, 5540–5541. [CrossRef]
31. Li, J.-L.; Segui, A.R. Surface plasmonic gold nanorods for enhanced two-photon microscopic imaging and apoptosis induction of cancer cells. Biomaterials 2010, 31, 9492–9498. [CrossRef]
32. Wang, H.; Huff, T.B.; Zweifel, D.A.; He, W.; Low, P.S.; Wei, A.; Cheng, J.-X. In vitro and in vivo two-photon luminescence imaging of single gold nanorods. Proc. Natl. Acad. Sci. USA 2005, 102, 15752–15756. [CrossRef]
33. Haran, G.; Chuntonov, L. Artificial Plasmonic Molecules and Their Interaction with Real Molecules. Chem. Rev. 2018, 118, 5539–5580. [CrossRef]
34. Huang, X.; El-Sayed, I.H.; Qian, W.; El-Sayed, M.A. Cancer Cell Imaging and Photothermal Therapy in the Near-Infrared Region by Using Gold Nanorods. J. Am. Chem. Soc. 2006, 128, 2115–2120. [CrossRef]
35. Weissleder, R. A clearer vision for in vivo imaging. Nat. Biotechnol. 2001, 19, 316–317. [CrossRef]
36. Huang, X.; El-Sayed, M.A. Plasmonic photo-thermal therapy (PPTT). Alex. J. Med. 2011, 47, 1–9. [CrossRef]
37. Pitsillides, C.M.; Joe, E.K.; Wei, X.; Anderson, R.R.; Lin, C.P. Selective Cell Targeting with Light-Absorbing Microparticles and Nanoparticles. Biophys. J. 2003, 84, 4023–4032. [CrossRef]
38. Hirsch, L.R.; Stafford, R.J.; Bankson, J.A.; Sershen, S.R.; Rivera, B.; Price, R.E.; Hazle, J.D.; Halas, N.J.; West, J.L. Nanoshell-mediated near-infrared thermal therapy of tumors under magnetic resonance guidance. Proc. Natl. Acad. Sci. USA 2003, 100, 13549–13554. [CrossRef]
39. O’Neal, D.P.; Hirsch, L.R.; Halas, N.J.; Payne, J.D.; West, J.L. Photo-thermal tumor ablation in mice using near infrared-absorbing nanoparticles. Cancer Lett. 2004, 209, 171–176. [CrossRef]
40. Nie, S. Editorial: Understanding and overcoming major barriers in cancer nanomedicine. Nanomedicine 2010, 5, 523–528. [CrossRef]
41. Ali, M.; Wu, Y.; El-Sayed, M.A. Gold-Nanoparticle-Assisted Plasmonic Photothermal Therapy Advances Toward Clinical Application. J. Phys. Chem. C 2019, 123, 15375–15393. [CrossRef]
42. Boyer, D.; Tamarat, P.; Maali, A.; Lounis, B.; Orrit, M. Photothermal Imaging of Nanometer-Sized Metal Particles Among Scatterers. Science 2002, 297, 1160–1163. [CrossRef]
43. Liu, Y.; Bhattarai, P.; Dai, Z.; Chen, X. Photothermal therapy and photoacoustic imaging via nanotheranostics in fighting cancer. Chem. Soc. Rev. 2019, 48, 2053–2108. [CrossRef]
44. Lucky, S.S.; Soo, K.C.; Zhang, Y. Nanoparticles in Photodynamic Therapy. Chem. Rev. 2015, 115, 1990–2042. [CrossRef]

45. Vijayaraghavan, P.; Liu, C.-H.; Vankayala, R.; Chiang, C.-S.; Hwang, K.C. Designing Multi-Branched Gold Nanoechinus for NIR Light Activated Dual Modal Photodynamic and Photothermal Therapy in the Second Biological Window. Adv. Mater. 2014, 26, 6689–6695. [CrossRef]
46. Jang, B.; Park, J.-Y.; Tung, C.-H.; Kim, I.-H.; Choi, Y. Gold Nanorod−Photosensitizer Complex for Near-Infrared Fluorescence Imaging and Photodynamic/Photothermal Therapy In Vivo. ACS Nano 2011, 5, 1086–1094. [CrossRef]
47. Vankayala, R.; Sagadevan, A.; Vijayaraghavan, P.; Kuo, C.-L.; Hwang, K.C. Metal Nanoparticles Sensitize the Formation of Singlet Oxygen. Angew. Chem. Int. Ed. 2011, 50, 10640–10644. [CrossRef]
48. Vankayala, R.; Huang, Y.-K.; Kalluru, P.; Chiang, C.-S.; Hwang, K.C. First Demonstration of Gold Nanorods-Mediated Photodynamic Therapeutic Destruction of Tumors via Near Infra-Red Light Activation. Small 2013, 10, 1612–1622. [CrossRef]
49. Ali, M.R.K.; Wu, Y.; El-Sayed, M.A. Gold-Nanoparticle-Assisted Plasmonic Photothermal Therapy Advances Toward Clinical Application. J. Phys. Chem. C 2019, 123, 15375–15393. [CrossRef]
50. Chen, Q.; Chen, J.; Yang, Z.; Zhang, L.; Dong, Z.; Liu, Z. NIR-II light activated photodynamic therapy with protein-capped gold nanoclusters. Nano Res. 2018, 11, 5657–5669. [CrossRef]
51. Vankayala, R.; Lin, C.-C.; Kalluru, P.; Chiang, C.-S.; Hwang, K.C. Gold nanoshells-mediated bimodal photodynamic and photothermal cancer treatment using ultra-low doses of near infra-red light. Biomaterials 2014, 35, 5527–5538. [CrossRef]
52. Gao, L.; Fei, J.; Zhao, J.; Li, H.; Cui, Y.; Li, J. Hypocrellin-Loaded Gold Nanocages with High Two-Photon Efficiency for Photothermal/Photodynamic Cancer Therapy in Vitro. ACS Nano 2012, 6, 8030–8040. [CrossRef]
53. Wang, S.; Huang, P.; Nie, L.; Xing, R.; Liu, D.; Wang, Z.; Lin, J.; Chen, S.; Niu, G.; Lu, G.M.; et al. Biomedical Applications: Single Continuous Wave Laser Induced Photodynamic/Plasmonic Photothermal Therapy Using Photosensitizer-Functionalized Gold Nanostars (Adv. Mater. 22/2013). Adv. Mater. 2013, 25, 3009. [CrossRef]
54. Kuo, W.-S.; Chang, Y.-T.; Cho, K.-C.; Chiu, K.-C.; Lien, C.-H.; Yeh, C.-S.; Chen, S.-J. Gold nanomaterials conjugated with indocyanine green for dual-modality photodynamic and photothermal therapy. Biomaterials 2012, 33, 3270–3278. [CrossRef]
55. Wang, B.; Wang, J.; Liu, Q.; Huang, H.; Chen, M.; Li, K.; Li, C.; Yu, X.; Chu, P.K. Rose-bengal-conjugated gold nanorods for in vivo photodynamic and photothermal oral cancer therapies. Biomaterials 2014, 35, 1954–1966. [CrossRef]
56. Wang, N.; Zhao, Z.; Lv, Y.; Fan, H.; Bai, H.; Meng, H.; Long, Y.; Fu, T.; Zhang, X.-B.; Tan, W. Gold nanorod-photosensitizer conjugate with extracellular pH-driven tumor targeting ability for photothermal/photodynamic therapy. Nano Res. 2014, 7, 1291–1301. [CrossRef]
57. Terentyuk, G.; Panfilova, E.; Khanadeev, V.; Chumakov, D.; Genina, E.; Bashkatov, A.; Tuchin, V.; Bucharskaya, A.; Maslyakova, G.; Khlebtsov, N.G.; et al. Gold nanorods with a hematoporphyrin-loaded silica shell for dual-modality photodynamic and photothermal treatment of tumors in vivo. Nano Res. 2014, 7, 325–337. [CrossRef]
58. Bucharskaya, A.; Maslyakova, G.; Terentyuk, G.; Yakunin, A.; Avetisyan, Y.; Bibikova, O.; Tuchina, E.; Khlebtsov, B.; Khlebtsov, N.G.; Tuchin, V.V. Towards Effective Photothermal/Photodynamic Treatment Using Plasmonic Gold Nanoparticles. Int. J. Mol. Sci. 2016, 17, 1295. [CrossRef]
59. Wang, J.; Chen, J.-Y. Synergistic effect to kill cancer cells by gold nanorod-aluminum phthalocyanine conjugates. In Proceedings of the 12th IEEE International Conference on Nanotechnology (IEEE-NANO), Birmingham, UK, 20–23 August 2012; pp. 1–3.
60. Jang, B.; Park, J.Y.; Tung, C.H.; Kim, I.H.; Choi, Y. Gold nanorod-photosensitizer complex for near-infrared fluorescence imaging and photodynamic/photothermal therapy in vivo. ACS Nano 2011, 5, 1086–1094. [CrossRef]
61. Yu, M.; Guo, F.; Wang, J.; Tan, F.; Li, N. Photosensitizer-Loaded pH-Responsive Hollow Gold Nanospheres for Single Light-Induced Photothermal/Photodynamic Therapy. ACS Appl. Mater. Interfaces 2015, 7, 17592–17597. [CrossRef]
62. Zhou, W.; Gao, X.; Liu, D.; Chen, X. Gold Nanoparticles for In Vitro Diagnostics. Chem. Rev. 2015, 115, 10575–10636. [CrossRef
63. Kang, J.-H.; Asami, Y.; Murata, M.; Kitazaki, H.; Sadanaga, N.; Tokunaga, E.; Shiotani, S.; Okada, S.; Maehara, Y.; Niidome, T. Gold nanoparticle-based colorimetric assay for cancer diagnosis. Biosens. Bioelectron. 2010, 25, 1869–1874. [CrossRef]
64. O'Brian, C.A.; Chu, F.; Bornmann, W.G.; Maxwell, D.S. Protein kinase Cα and ε small-molecule targeted therapeutics: A new roadmap to two Holy Grails in drug discovery? Expert Rev. Anticancer. Ther. 2006, 6, 175–186. [CrossRef]
65. Lu, W.; Arumugam, S.R.; Senapati, D.; Singh, A.K.; Arbneshi, T.; Khan, S.A.; Yu, H.; Ray, P.C.; Yu, S.A.K.H. Multifunctional Oval-Shaped Gold-Nanoparticle-Based Selective Detection of Breast Cancer Cells Using Simple Colorimetric and Highly Sensitive Two-Photon Scattering Assay. ACS Nano 2010, 4, 1739–1749. [CrossRef]
66. Oh, J.-H.; Lee, J.-S. Designed Hybridization Properties of DNA–Gold Nanoparticle Conjugates for the Ultraselective Detection of a Single-Base Mutation in the Breast Cancer GeneBRCA1. Anal. Chem. 2011, 83, 7364–7370. [CrossRef]

67. Ramanathan, S.; Gopinath, S.C.B.; Arshad, M.K.M.; Poopalan, P.; Anbu, P. A DNA based visual and colorimetric aggregation assay for the early growth factor receptor (EGFR) mutation by using unmodified gold nanoparticles. Microchim. Acta 2019, 186, 546. [CrossRef]
68. Valentini, P.; Fiammengo, R.; Sabella, S.; Gariboldi, M.; Maiorano, G.; Cingolani, R.; Pompa, P.P. Gold-Nanoparticle-Based Colorimetric Discrimination of Cancer-Related Point Mutations with Picomolar Sensitivity. ACS Nano 2013, 7, 5530–5538. [CrossRef]
69. Assah, E.; Goh, W.; Zheng, X.T.; Lim, T.X.; Li, J.; Lane, D.P.; Ghadessy, F.; Tan, Y.N. Rapid colorimetric detection of p53 protein function using DNA-gold nanoconjugates with applications for drug discovery and cancer diagnostics. Colloids Surf. B Biointerfaces 2018, 169, 214–221. [CrossRef]
70. Huang, J.; Liou, Y.L.; Kang, Y.N.; Tan, Z.R.; Peng, M.J.; Zhou, H.H. Real-time colorimetric detection of DNA methylation of the PAX1 gene in cervical scrapings for cervical cancer screening with thiol-labeled PCR primers and gold nanoparticles. Int. J. Nanomed. 2016, 11, 5335–5347. [CrossRef]
71. Berning, D.E.; Katti, K.V.; Volkert, W.A.; Higginbotham, C.J.; Ketring, A.R. 198Au-labeled hydroxymethyl phosphines as models for potential therapeutic pharmaceuticals. Nucl. Med. Boil. 1998, 25, 577–583. [CrossRef]
72. Fent, G.M.; Casteel, S.W.; Kim, D.Y.; Kannan, R.; Katti, K.; Chanda, N.; Katti, K. Biodistribution of maltose and gum arabic hybrid gold nanoparticles after intravenous injection in juvenile swine. Nanomed. Nanotechnol. Boil. Med. 2009, 5, 128–135. [CrossRef]
73. Curran, W.J.; Littman, P.; Raney, R.B. Interstitial radiation therapy in the treatment of childhood soft-tissue sarcomas. Int. J. Radiat. Oncol. 1988, 14, 169–174. [CrossRef]
74. Cutler, C.S.; Hennkens, H.M.; Sisay, N.; Huclier-Markai, S.; Jurisson, S. Radiometals for Combined Imaging and Therapy. Chem. Rev. 2012, 113, 858–883. [CrossRef]
75. Rich, T.A. Radiation therapy for pancreatic cancer: Eleven year experience at the JCRT. Int. J. Radiat. Oncol. 1985, 11, 759–763. [CrossRef]
76. Chanda, N.; Kan, P.; Watkinson, L.D.; Shukla, R.; Zambre, A.; Carmack, T.L.; Engelbrecht, H.; Lever, J.R.; Katti, K.; Fent, G.M.; et al. Radioactive gold nanoparticles in cancer therapy: Therapeutic efficacy studies of GA-198AuNP nanoconstruct in prostate tumor-bearing mice. Nanomed. Nanotechnol. Boil. Med. 2010, 6, 201–209. [CrossRef]
77. Floyd, C.E.; Jaszczak, R.J.; Harris, C.C.; Coleman, R.E. Energy and spatial distribution of multiple order Compton scatter in SPECT: A Monte Carlo investigation. Phys. Med. Boil. 1984, 29, 1217–1230. [CrossRef]
78. Knight, P.J.; Doornbos, J.F.; Rosen, D.; Lin, J.J.; Farha, G.J. The use of interstitial radiation therapy in the treatment of persistent, localized, and unresectable cancer in children. Cancer 1986, 57, 951–954. [CrossRef]
79. Chen, C.-H.; Lin, F.-S.; Liao, W.-N.; Liang, S.L.; Chen, M.-H.; Chen, Y.-W.; Lin, W.-Y.; Hsu, M.-H.; Wang, M.-Y.; Peir, J.-J.; et al. Establishment of a Trimodality Analytical Platform for Tracing, Imaging and Quantification of Gold Nanoparticles in Animals by Radiotracer Techniques. Anal. Chem. 2014, 87, 601–608. [CrossRef]
80. Wang, Y.; Liu, Y.; Luehmann, H.; Xia, X.; Wan, D.; Cutler, C.; Xia, Y. Radioluminescent Gold Nanocages with Controlled Radioactivity for Real-Time in Vivo Imaging. Nano Lett. 2013, 13, 581–585. [CrossRef]
81. Guo, Y.; Aweda, T.; Black, K.C.; Liu, Y. Chemistry and Theranostic Applications of Radiolabeled Nanoparticles for Cardiovascular, Oncological, and Pulmonary Research. Curr. Top. Med. Chem. 2013, 13, 470–478.
82. Yaal-Hahoshen, N.; Shina, S.; Leider-Trejo, L.; Barnea, I.; Shabtai, E.L.; Azenshtein, E.; Greenberg, I.; Keydar, I.; Ben-Baruch, A. The Chemokine CCL5 as a Potential Prognostic Factor Predicting Disease Progression in Stage II Breast Cancer Patients. Clin. Cancer Res. 2006, 12, 4474–4480. [CrossRef] [PubMed]
83. Fazaeli, Y.; Akhavan, O.; Rahighi, R.; Aboudzadeh, M.R.; Karimi, E.; Afarideh, H. In vivo SPECT imaging of tumors by 198,199Au-labeled graphene oxide nanostructures. Mater. Sci. Eng. C 2014, 45, 196–204. [CrossRef] [PubMed]
84. Hainfeld, J.F. Gold cluster-labelled antibodies. Nature 1988, 333, 281–282. [CrossRef] [PubMed]
85. Payton, S. Prostate cancer: Radioactive gold nanoparticles show promise for tumour shrinkage. Nat. Rev. Urol. 2012, 9, 544. [CrossRef] [PubMed]
86. Matsudaira, H.; Ueno, A.M.; Furuno, I. Iodine contrast medium sensitizes cultured mammalian cells to X rays but not to gamma rays. Radiat. Res. 1980, 84, 144–148. [CrossRef] [PubMed]
87. Hernandez-Rivera, M.; Kumar, I.; Cho, S.Y.; Cheong, B.Y.; Pulikkathara, M.X.; Moghaddam, S.E.; Whitmire, K.H.; Wilson, L.J. High-Performance Hybrid Bismuth-Carbon Nanotube Based Contrast Agent for X-ray CT Imaging. Acs Appl. Mater. Interfaces 2017, 9, 5709–5716. [CrossRef] [PubMed]
88. Seltzer, S.M. Tables of X-Ray Mass Attenuation Coefficients and Mass Energy–Absorption Coefficients NISTIR 5632. Pramana 1995, 72, 375–387.
89. Leung, M.K.K.; Chow, J.C.L.; Chithrani, D.; Lee, M.J.G.; Oms, B.; Jaffray, D. Irradiation of gold nanoparticles by X-rays: Monte Carlo simulation of dose enhancements and the spatial properties of the secondary electrons production. Med Phys. 2011, 38, 624. [CrossRef]
90. Carter, J.D.; Cheng, N.N.; Qu, Y.; Suarez, G.D.; Guo, T. Nanoscale Energy Deposition by X-ray Absorbing Nanostructures. J. Phys. Chem. B 2007, 111, 11622–11625. [CrossRef]

91. Michael, D.; Eva, B.; Scott, P. Monte Carlo investigation of the increased radiation deposition due to gold nanoparticles using kilovoltage and megavoltage photons in a 3D randomized cell model. Med. Phys. 2013, 40, 071710.
92. Kwatra, D.; Venugopal, A.; Anant, S. Nanoparticles in radiation therapy: A summary of various pproaches to enhance radiosensitization in cancer. Transl. Cancer Res. 2013, 2, 330–342.
93. Wu, L.-J.; Randers-Pehrson, G.; Xu, A.; Waldren, C.A.; Geard, C.R.; Yu, Z.; Hei, T.K. Targeted cytoplasmic irradiation with alpha particles induces mutations in mammalian cells. Proc. Natl. Acad. Sci. USA 1999, 96, 4959–4964. [CrossRef] [PubMed]
94. Berbeco, R.; Ngwa, W.; Makrigiorgos, G.M. Localized Dose Enhancement to Tumor Blood Vessel Endothelial Cells via Megavoltage X-rays and Targeted Gold Nanoparticles: New Potential for External Beam Radiotherapy. Int. J. Radiat. Oncol. 2011, 81, 270–276. [CrossRef] [PubMed]
95. Her, S.; Jaffray, D.; Allen, C. Gold nanoparticles for applications in cancer radiotherapy: Mechanisms and recent advancements. Adv. Drug Deliv. Rev. 2017, 109, 84–101. [CrossRef] [PubMed]
96. Brun, E.; Sanche, L.; Sicard-Roselli, C. Parameters governing gold nanoparticle X-ray radiosensitization of DNA in solution. Colloids Surf. B Biointerfaces 2009, 72, 128–134. [CrossRef] [PubMed]
97. Hyun, C.S.; Jones, B.L.; Sunil, K. The dosimetric feasibility of gold nanoparticle-aided radiation therapy (GNRT) via brachytherapy using low-energy gamma-/x-ray sources. Phys. Med. Biol. 2009, 54, 4889.
98. Lechtman, E.; Chattopadhyay, N.; Cai, Z.; Mashouf, S.; Reilly, R.; Pignol, J.P. Implications on clinical scenario of gold nanoparticle radiosensitization in regards to photon energy, nanoparticle size, concentration and location. Phys. Med. Boil. 2011, 56, 4631–4647. [CrossRef]
99. Alqathami, M.; Blencowe, A.; Yeo, U.J.; Doran, S.J.; Qiao, G.; Geso, M. Novel multicompartment 3-dimensional radiochromic radiation dosimeters for nanoparticle-enhanced radiation therapy dosimetry. Int. J. Radiat. Oncol. Biol. Phys. 2012, 84, e549–e555. [CrossRef]
100. Hainfeld, J.F.; Slatkin, D.N.; Smilowitz, H.M. The use of gold nanoparticles to enhance radiotherapy in mice. Phys. Med. Boil. 2004, 49, N309–N315. [CrossRef]
101. Popovtzer, R.; Agrawal, A.; Kotov, N.A.; Popovtzer, A.; Balter, J.; Carey, T.E.; Kopelman, R. Targeted gold nanoparticles enable molecular CT imaging of cancer. Nano Lett. 2008, 8, 4593–4596. [CrossRef]
102. Popovtzer, R.; Reuveni, T.; Motiei, M.; Romman, Z.; Popovtzer, A. Targeted gold nanoparticles enable molecular CT imaging of cancer: An in vivo study. Int. J. Nanomed. 2011, 6, 2859–2864. [CrossRef] [PubMed]
103. Jans, H.; Huo, Q. Gold nanoparticle-enabled biological and chemical detection and analysis. Chem. Soc. Rev. 2012, 41, 2849–2866. [CrossRef
104. Perrault, S.D.; Walkey, C.; Jennings, T.; Fischer, H.C.; Chan, W.C.W. Mediating Tumor Targeting Efficiency of Nanoparticles Through Design. Nano Lett. 2009, 9, 1909–1915. [CrossRef] [PubMed]
105. Sykes, E.A.; Chen, J.; Zheng, G.; Chan, W.C. Investigating the Impact of Nanoparticle Size on Active and Passive Tumor Targeting Efficiency. ACS Nano 2014, 8, 5696–5706. [CrossRef] [PubMed]
106. Chou, L.Y.T.; Chan, W.C.W. Fluorescence-Tagged Gold Nanoparticles for Rapidly Characterizing the Size-Dependent Biodistribution in Tumor Models. Adv. Heal. Mater. 2012, 1, 714–721. [CrossRef]
107. Blanco, E.; Shen, H.; Ferrari, M. Principles of nanoparticle design for overcoming biological barriers to drug delivery. Nat. Biotechnol. 2015, 33, 941–951. [CrossRef]
108. Bai, X.; Zhang, J.; Chang, Y.-N.; Gu, W.; Lei, R.; Qin, Y.; Xia, S.; Ma, S.; Liang, Y.; Chen, K.; et al. Nanoparticles with High-Surface Negative-Charge Density Disturb the Metabolism of Low-Density Lipoprotein in Cells. Int. J. Mol. Sci. 2018, 19, 2790. [CrossRef] [PubMed]
109. Chen, Y.-S.; Hung, Y.-C.; Liau, I.; Huang, G.S. Assessment of the In Vivo Toxicity of Gold Nanoparticles. Nanoscale Res. Lett. 2009, 4, 858–864. [CrossRef] [PubMed]
110. Zhou, C.; Long, M.; Qin, Y.; Sun, X.; Zheng, J. Luminescent Gold Nanoparticles with Efficient Renal Clearance. Angew. Chem. Int. Ed. 2011, 50, 3168–3172. [CrossRef] [PubMed]
111. Cho, W.-S.; Cho, M.; Jeong, J.; Choi, M.; Han, B.-S.; Shin, H.-S.; Hong, J.; Chung, B.H.; Jeong, J.; Cho, M.-H. Size-dependent tissue kinetics of PEG-coated gold nanoparticles. Toxicol. Appl. Pharmacol. 2010, 245, 116–123. [CrossRef] [PubMed]
112. Khlebtsov, N.; Dykman, L. Biodistribution and toxicity of engineered gold nanoparticles: A review of in vitro and in vivo studies. Chem. Soc. Rev. 2011, 40, 1647–1671. [CrossRef] [PubMed]
113. Iyer, A.K.; Khaled, G.; Fang, J.; Maeda, H. Exploiting the enhanced permeability and retention effect for tumor targeting. Drug Discov. Today 2006, 11, 812–818. [CrossRef] [PubMed]
114. Zhang, X.-D.; Wu, D.; Shen, X.; Chen, J.; Sun, Y.-M.; Liu, P.-X.; Liang, X.-J. Size-dependent radiosensitization of PEG-coated gold nanoparticles for cancer radiation therapy. Biomaterials 2012, 33, 6408–6419. [CrossRef] [PubMed]
115. Piao, J.; Wang, L.; Gao, F.; You, Y.-Z.; Xiong, Y.; Yang, L. Erythrocyte Membrane Is an Alternative Coating to Polyethylene Glycol for Prolonging the Circulation Lifetime of Gold Nanocages for Photothermal Therapy. ACS Nano 2014, 8, 10414–10425. [CrossRef] [PubMed]

116. Al Zaki, A.; Joh, D.; Cheng, Z.; De Barros, A.L.B.; Kao, G.; Dorsey, J.; Tsourkas, A. Gold-Loaded Polymeric Micelles for Computed Tomography-Guided Radiation Therapy Treatment and Radiosensitization. ACS Nano 2014, 8, 104–112. [CrossRef]
117. Goy-López, S.; Castro, E.; Taboada, P.; Mosquera, V. Block Copolymer-Mediated Synthesis of Size-Tunable Gold Nanospheres and Nanoplates. Langmuir 2008, 24, 13186–13196. [CrossRef]
118. Chanda, N.; Kattumuri, V.; Shukla, R.; Zambre, A.; Katti, K.; Upendran, A.; Kulkarni, R.R.; Kan, P.; Fent, G.M.; Casteel, S.W.; et al. Bombesin functionalized gold nanoparticles show in vitro and in vivo cancer receptor specificity. Proc. Natl. Acad. Sci. USA 2010, 107, 8760–8765. [CrossRef]
119. Yuan, H.; Fales, A.M.; Vo-Dinh, T. TAT Peptide-Functionalized Gold Nanostars: Enhanced Intracellular Delivery and Efficient NIR Photothermal Therapy Using Ultralow Irradiance. J. Am. Chem. Soc. 2012, 134, 11358–11361. [CrossRef]
120. Kim, J.; Park, S.; Lee, J.E.; Jin, S.M.; Lee, J.H.; Lee, I.S.; Yang, I.; Kim, J.-S.; Kim, S.K.; Cho, M.-H.; et al. Designed Fabrication of Multifunctional Magnetic Gold Nanoshells and Their Application to Magnetic Resonance Imaging and Photothermal Therapy. Angew. Chem. Int. Ed. 2006, 45, 7754–7758. [CrossRef]
121. Dumani, D.S.; Sun, I.-C.; Emelianov, S.Y. Ultrasound-guided immunofunctional photoacoustic imaging for diagnosis of lymph node metastases. Nanoscale 2019, 11, 11649–11659. [CrossRef]
122. Xianyu, Y.; Xie, Y.; Wang, N.; Wang, Z.; Jiang, X. A Dispersion-Dominated Chromogenic Strategy for Colorimetric Sensing of Glutathione at the Nanomolar Level Using Gold Nanoparticles. Small 2015, 11, 5510–5514. [CrossRef] [PubMed]
123. Tian, F.; Conde, J.; Bao, C.; Chen, Y.; Curtin, J.F.; Cui, D. Gold nanostars for efficient in vitro and in vivo real-time SERS detection and drug delivery via plasmonic-tunable Raman/FTIR imaging. Biomaterials 2016, 106, 87–97. [CrossRef] [PubMed]
124. Cheng, Y.; Samia, A.C.; Meyers, J.D.; Panagopoulos, I.; Fei, B.; Burda, C. Highly Efficient Drug Delivery with Gold Nanoparticle Vectors for in Vivo Photodynamic Therapy of Cancer. J. Am. Chem. Soc. 2008, 130, 10643–10647. [CrossRef] [PubMed
125. Li, G.; Chen, Y.; Zhang, L.; Zhang, M.; Li, S.; Li, L.; Wang, T.; Wang, C. Facile Approach to Synthesize Gold Nanorod@Polyacrylic Acid/Calcium Phosphate Yolk–Shell Nanoparticles for Dual-Mode Imaging and pH/NIR-Responsive Drug Delivery. Nano-Micro Lett. 2017, 10, 7. [CrossRef] [PubMed]
126. Anderson, P.; Vaughan, A.T.; Varley, N.R. Antibodies labeled with 199Au: Potential of 199Au for radioimmunotherapy. Int. J. Radiat. Appl. Instrum. Part B Nucl. Med. Boil. 1988, 15, 293–297. [CrossRef]
127. Luo, C.; Wen, W.; Lin, F.; Zhang, X.; Gu, H.; Wang, S. Simplified aptamer-based colorimetric method using unmodified gold nanoparticles for the detection of carcinoma embryonic antigen. RSC Adv. 2015, 5, 10994–10999. [CrossRef]
128. Hainfeld, J. A small gold-conjugated antibody label: Improved resolution for electron microscopy. Science 1987, 236, 450–453. [CrossRef]
129. Lin, Y.; Ren, J.; Qu, X. Nano-Gold as Artificial Enzymes: Hidden Talents. Adv. Mater. 2014, 26, 4200–4217. [CrossRef]
130. Jv, Y.; Li, B.; Cao, R. Positively-charged gold nanoparticles as peroxidiase mimic and their application in hydrogen peroxide and glucose detection. Chem. Commun. 2010, 46, 8017. [CrossRef]
131. Zhang, A.; Pan, S.; Zhang, Y.; Chang, J.; Cheng, J.; Huang, Z.; Li, T.; Zhang, C.; De La Fuentea, J.M.; Zhang, Q.; et al. Carbon-gold hybrid nanoprobes for real-time imaging, photothermal/photodynamic and nanozyme oxidative therapy. Theranostics 2019, 9, 3443–3458. [CrossRef]
132. Feng, J.; Huang, P.; Shi, S.; Deng, K.-Y.; Wu, F.-Y. Colorimetric detection of glutathione in cells based on peroxidase-like activity of gold nanoclusters: A promising powerful tool for identifying cancer cells. Anal. Chim. Acta 2017, 967, 64–69. [CrossRef] [PubMed]
133. Comotti, M.; Della Pina, C.; Matarrese, R.; Rossi, M. The Catalytic Activity of "Naked" Gold Particles. Angew. Chem. Int. Ed. 2004, 43, 5812–5815. [CrossRef] [PubMed]
134. Liu, D.; Yang, J.; Wang, H.-F.; Wang, Z.; Huang, X.; Wang, Z.; Niu, G.; Walker, A.R.H.; Chen, X. Glucose Oxidase-Catalyzed Growth of Gold Nanoparticles Enables Quantitative Detection of Attomolar Cancer Biomarkers. Anal. Chem. 2014, 86, 5800–5806. [CrossRef] [PubMed]
135. Gao, S.; Lin, H.; Zhang, H.; Yao, H.; Chen, Y.; Shi, J. Nanocatalytic Tumor Therapy by Biomimetic Dual Inorganic Nanozyme-Catalyzed Cascade Reaction. Adv. Sci. 2018, 6, 1801733. [CrossRef]
136. Pan, Y.; Leifert, A.; Ruau, D.; Neuss, S.; Bornemann, J.; Schmid, G.; Brandau, W.; Simon, U.; Jahnen-Dechent, W. Gold Nanoparticles of Diameter 1.4 nm Trigger Necrosis by Oxidative Stress and Mitochondrial Damage. Small 2009, 5, 2067–2076. [CrossRef]
137. Mukherjee, P.; Bhattacharya, R.; Wang, P.; Wang, L.; Basu, S.; Nagy, J.A.; Atala, A.; Mukhopadhyay, D.; Soker, S. Antiangiogenic Properties of Gold Nanoparticles. Clin. Cancer Res. 2005, 11, 3530–3534. [CrossRef]

138. Bhattacharya, R.; Patra, C.R.; Verma, R.; Kumar, S.; Greipp, P.R.; Mukherjee, P. Gold Nanoparticles Inhibit the Proliferation of Multiple Myeloma Cells. Adv. Mater. 2007, 19, 711–716. [CrossRef]
139. Wang, L.; Liu, Y.; Li, W.; Jiang, X.; Ji, Y.; Wu, X.; Xu, L.; Qiu, Y.; Zhao, K.; Wei, T.; et al. Selective Targeting of Gold Nanorods at the Mitochondria of Cancer Cells: Implications for Cancer Therapy. Nano Lett. 2011, 11, 772–780. [CrossRef]